



New Approaches in Nondestructive Characterisation of the Interface in Metal - CFRP Hybrid Structures

Hans-Georg HERRMANN¹, Michael SCHWARZ², Jannik SUMMA²

¹ Fraunhofer-Institut für Zerstörungsfreie Prüfverfahren IZFP, Saarbrücken, Germany

² Universität des Saarlandes, Saarbrücken, Germany

Contact e-mail: hans-georg.herrmann@izfp.fraunhofer.de

Abstract. With regard to cost-efficient lightweight design there is an obvious trend to join different materials resulting in hybrid structures, such as joining metal with CFRP (Carbon Fibre Reinforced Polymer) structures. In order to reduce the gap in stiffness between the metal and CFRP structure a thermoplastic polymer component can be inserted, which is capable to fulfil additional functional properties.

To characterise the used materials and defects in the hybrid, nondestructive testing (NDT) approaches in combination with mechanical testing are shown. Especially the interface between the metal structure and the thermoplastic polymer component as well as the interface between the thermoplastic polymer component and the CFRP structure are investigated because previous works have shown for adhesively joints that cracks initialising within the adhesive zone lead to ultimate failure by fracture of the CFRP ply adjacent to the adhesive. Thus ultimate failure of the hybrid joint is significantly determined by the crack resistance of the CFRP.

Therefore investigations will be presented with active thermography and ultrasonic (US) testing on CFRP samples with defined defects, which are artificially implanted within the preforming process. Furthermore passive thermography during mechanical testing will be applied to characterise the effect of the artificial defects in the CFRP samples whilst loading. By combining different NDT methods, the characterisation of defects shall be improved. Additionally electromagnetic acoustic transducers (EMAT) are used to evaluate the quality of the adhesive bonding of the metal and the thermoplastic polymer component.

Introduction

With increasing application of metal to CFRP hybrid-joints, problems with impeded lifecycle assessment arise, since various damage mechanisms may occur within the CFRP [1]. Moreover the damage propagation is partially unknown for different kinds of force-coupling at the interfaces [2]. Therefore relatively high effort applying nondestructive testing is required in order to assess the quality and the lifetime to failure.

In terms of quality assessment the main objective is to detect existing flaws with subsequent evaluation of their severity, which is mainly focused on the joining zone between the two components, as the discontinuity in mechanical properties causes structural attenuations [3] and the appearance of production induced defects may be promoted in this region.

In this work mechanical and nondestructive testing was carried out on $[0^\circ/90^\circ, \pm 45^\circ]_s$ CFRP samples containing 30 vol% of a 3K plain weave (Torayca FT300B)



embedded in the epoxy matrix (Biresin CR170/CH150-3). To validate the nondestructive testing methods artificial defects are implemented into the CFRP component within the Resin-Transfer-Moulding (RTM) -process. According to DIN EN ISO 527-4:1997, sample type 2, the geometrical parameters were chosen to be 120 mm length, 20 mm width and 1 mm thickness. The clamping length was chosen 25 mm on each side.

As nondestructive testing method active and passive thermography are chosen. Additionally aluminium-CFRP-bonding samples are characterised by ultrasonic testing.

1. Active Thermography

Active thermography needs an external excitation to achieve a thermal contrast. As excitation source halogen lamps, ultrasonic, eddy current, laser or flash generators can be used. To capture the thermal radiation after the sample is excited, an infrared camera is utilised. The used infrared camera is a so-called Dualband camera which is able to capture radiation from two spectral ranges. The spectral ranges are the midwave (4.4 – 5.2 μ m) and the longwave (7.8 – 8.8 μ m) infrared. Since defects act like thermal barriers they are depicted as bright areas in the infrared image. In the following infrared pictures CFRP samples with and without artificial defects are shown.

In Fig. 1 the front and rear side of a sample without artificial defect after mechanical testing is depicted. As you can see there are bright areas in the upper area of the sample. These bright areas represent delamination because of the mechanical testing. Furthermore the orientation of the inner layers ($\pm 45^\circ$) of the carbon fibres can be detected.

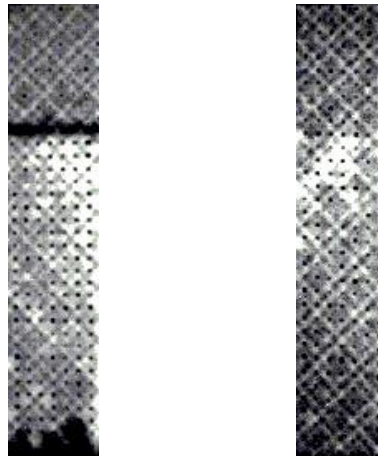


Fig. 1. Infrared picture of front (left) and rear side (right) of a CFRP-sample after mechanical testing.

In Fig. 2 an infrared picture of a sample with the artificial defect delamination, which should imitate an interface, is shown after mechanical testing. The artificial implemented defect is in the middle of the sample. As you can see there is also a crack at the upper side of the delamination. So the delamination acts as a weak point in the sample structure. This is also said in the work of Casas-Rodriguez [4].

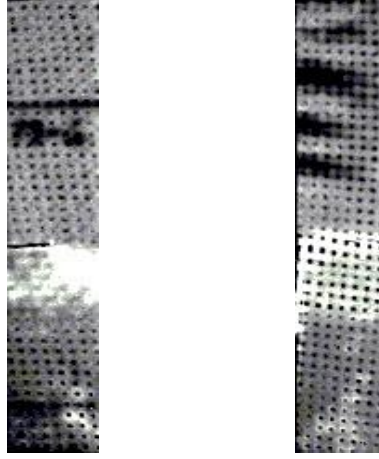


Fig. 2. Infrared picture of front (left) and rear (right) side of a CFRP-sample with artificial delamination after mechanical testing.

2. Passive thermography damage monitoring

Besides active thermography techniques with several excitation methods, passive thermography can be applied for *in situ* damage monitoring, as friction and deformation processes cause internal heat dissipation within the material. Thereby caused temperature variations can be expressed as a superposition of thermoelastic temperature variation ΔT_{el} , heat dissipation ΔT_{diss} and heat exchange with the environment ΔT_{loss} . It follows as reported by Rösner and Netzelmann [5]:

$$\begin{aligned}\Delta T(t) &= T(t) - T_0 \\ &= \Delta T_{el}(t) + \Delta T_{diss}(t) + \Delta T_{loss}(t)\end{aligned}\quad (1)$$

Where ΔT is the total temperature change and T_0 the absolute reference temperature at $t=0$.

The application of techniques like MIDA (mechanical induced heat dissipation) or TSA (thermal stress analysis) on carbon-fibre-reinforced-polymers is highly sophisticated, since low thermal conductivity, high heat capacity and high emissivity contribute to a good resolution. The emissivity of a surface is defined as [6]:

$$\varepsilon(\lambda, T, \theta', \phi') = \frac{L'_\lambda(\lambda, T, \theta', \phi')}{L_{\lambda,b}(\lambda, T)} \quad (2)$$

With L'_λ being the spectral radiance of a surface and $L_{\lambda,b}$ the spectral radiance of the black body.

It has been shown that passive thermography damage monitoring improves the capabilities characterising the damage progression under mechanical loadings. In [7], the methodology was used investigating the damage development of CFRP samples in tensile tests by means of the spontaneous temperature increase at the locus of fracture. Following the Clausius-Duhem inequality, [8] developed the local heat conduction equation as:

$$\rho C_{\varepsilon,\alpha} \frac{dT}{dt} + \text{div} \underline{q} = d_1 + \rho T \psi_{,T,\varepsilon} : \frac{d\varepsilon}{dt} + \rho T \psi_{,T,\alpha} \cdot \frac{d\alpha}{dt} + r_e \quad (3)$$

With ρ : density, $C_{\varepsilon,\alpha}$: specific heat capacity at constant ε and α , \mathbf{q} : heat influx vector, d_1 : intrinsic thermal dissipation, ψ : Helmholtz free energy, r_e : external heat supply, ε : strain, α : state variable.

In this work a good correlation between the spontaneous temperature increase due to fracture and the strain energy density and tensile strength respectively could be found for CFRP specimens containing different types of defects, e.g. gapping, pleat and delamination.

Table 1. Strain Energy Density (E_D), Temperature increase (ΔT) and Tensile Strength (σ_c) for CFRP specimens containing different defects

Pleat			Delamination			Defect-Free		
E_D [J/mm ³]	ΔT [K]	σ_c [MPa]	E_D [J/mm ³]	ΔT [K]	σ_c [MPa]	E_D [J/mm ³]	ΔT [K]	σ_c [MPa]
1,494	4,2	223,3	1,551	8,9	184,9	2,6	10,3	260

The differential temperature images of the fracture of CFRP samples corresponding to Table 1 are given in Fig. 3.

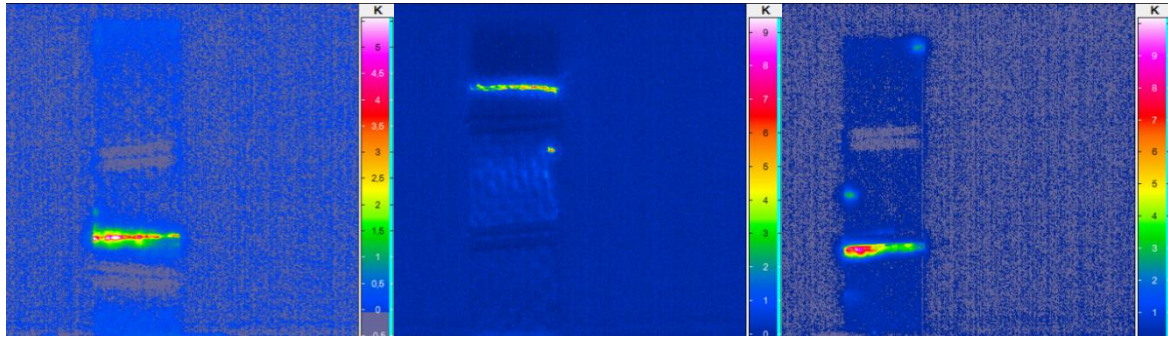


Fig. 3. Differential temperature image of passive Thermography of fracture of CFRP specimens a) with pleat b) with delamination c) defect-free; for better identification a grey isothermal is implemented for $\Delta T \leq 0$.

For passive thermography damage monitoring during fatigue experiments the dissipative heating has to be considered. Jegou [9] used a simplified relation of equation (3) to predict the Wöhler-curve from heat build-up measurements:

$$\rho C_{\varepsilon,\alpha} \frac{dT}{dt} - \lambda \Delta T = d_1 + \rho T \underline{k} : \frac{d\varepsilon^e}{dt} + r_e \quad (4)$$

Again, ρ : density, $C_{\varepsilon,\alpha}$: specific heat capacity at constant ε and α , d_1 : intrinsic thermal dissipation, \underline{k} : thermoelastic tensor, r_e : external heat supply, ε : strain.

Arif [10] demonstrated that the stiffness degradation of FRP during fatigue experiments comes along with an increase in maximum strain and an increasing of the average specimen temperature. Fig. 4 shows likewise investigations on CFRP samples, as a good agreement of the stiffness degradation and the temperature increase can be seen.

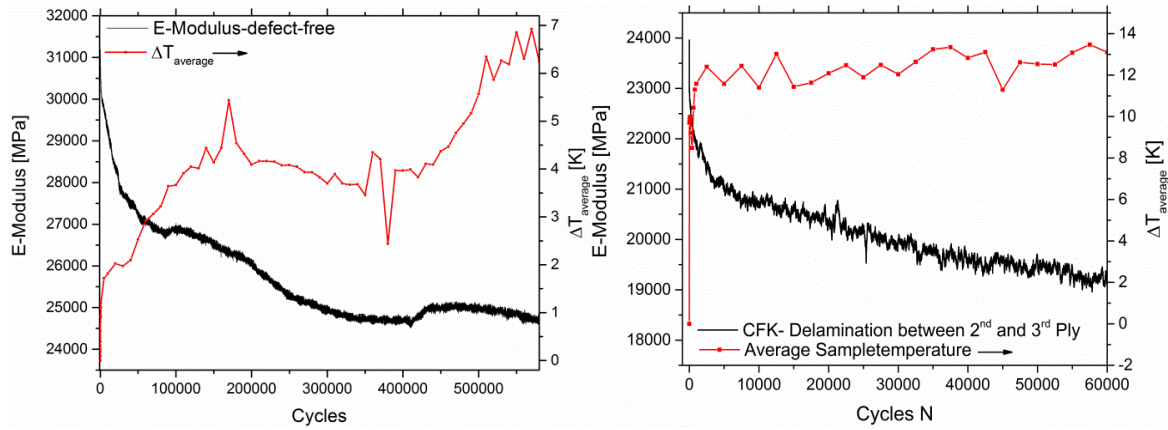


Fig. 4. Fatigue experiments: displacement controlled, $f=5$ Hz, displacement-ratio $r=0.1$ a) maximum displacement of 0,805 mm on a defect-free sample and b) maximum displacement of 0,60 mm on a sample with delamination. Left scale: degradation of E-Modulus, right scale: increase of average sample temperature.

The increase in average sample temperature provides information on the accumulated irreversible strains, whereas analysing the lateral temperature distribution depicts information on the damaged areas. Fig. 5 shows the difference of damage characterisation by means of thermal image (differential T-image) and by lock-in transformed amplitude image for a delaminated sample.

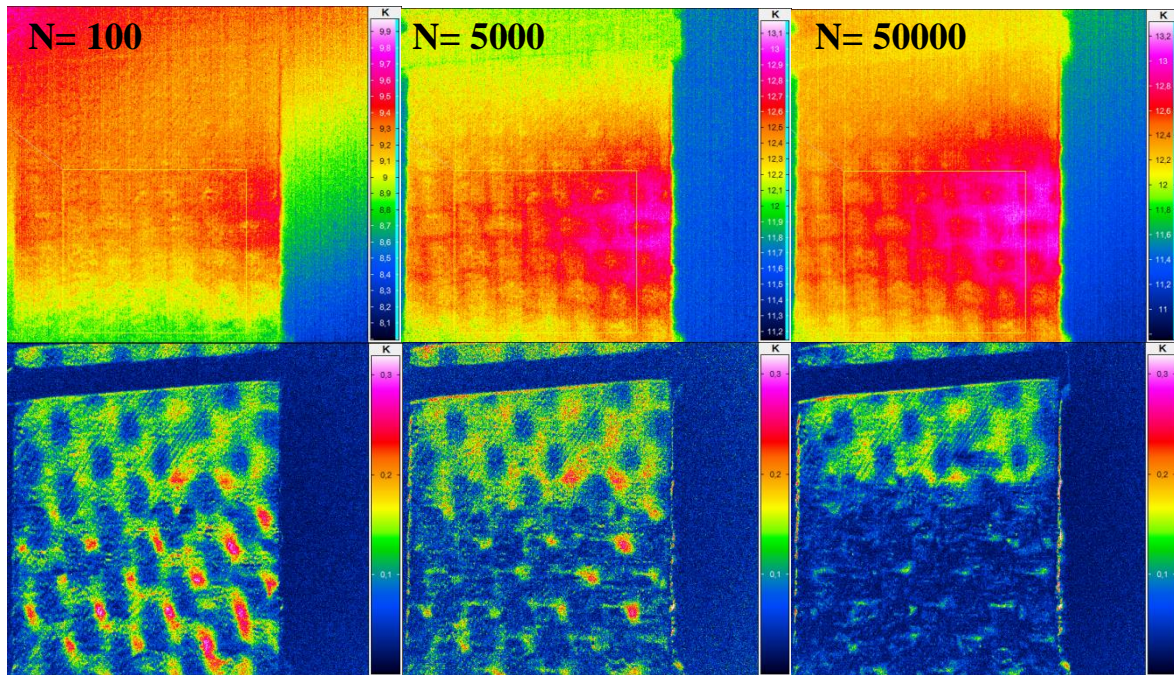


Fig. 5. Upper row: differential T-image referring to the image at $t=0$, lower row: corresponding lock-in transformed amplitude images for 5 Hz mechanical excitation and 30 Hz fps, left: 100 cycles, middle: 5000 cycles, right: $5 \cdot 10^4$ Cycles

It is evident from Fig. 3 that the hot spot revealed by thermal image, coincides with the most disturbed area in the lock-in transformed images. These observations indicate that the combination of both contrasts, differential T-image and lock-in transformed image, provide more information on the damage state of a specimen.

Additionally the combination of active and passive gives all information about a sample before, during and after mechanical testing. Fig. 2 and Fig. 5 show the same sample during and after mechanical testing. You can exactly describe the development of heat in the sample and can give a statement of the weak points in the sample structure.

3. Ultrasonic SH-waves

In addition to the already shown testing methods, there is a further method that is used to characterise the CFRP samples. This method uses Shear Horizontal Guided Waves (SH-waves) which are a special form of ultrasonic waves propagating in plates. To use SH-waves special transducers so-called electromagnetic acoustic transducers (EMAT) are needed. The waves are excited in the material either by the Lorentz force or by magnetostriction. For this reason the sample either has to be conductive or ferromagnetic. To achieve the effect of the Lorentz force, the material has to be conductive. In this case special induction coils are used. These induction coils are passed by a current impulse and induce eddy currents in the windings. By overlapping a magnetic field perpendicular to the surface with these generated eddy currents, periodic alternately Lorentz forces will appear. These Lorentz forces induce particle deflection acting as sources of ultrasonic waves in the material [11] (see Fig. 6).

To get the effect of magnetostriction, the used material has to be ferromagnetic. Whilst applying an external magnetic field, a ferromagnetic material will create a mechanical deformation, similar to the piezoelectric effect. The deformation occurs parallel to the applied magnetic field. Despite the eddy current in the material, dynamic magnetic fields are also induced, which create dynamic forces. These dynamic forces are parallel to the external magnetic flux.

The oscillation of the lattice atoms happens throughout the whole thickness of the plate, if it is in the dimension of or less the ultrasonic wavelength. This vibration propagates along the plate's length and is reflected at sharp edges, i.e. at the end of the plate. The advantage of this EMAT is the couplant free and contactless measurement. By using surface acoustic waves with this kind of ultrasonic testing, the interface between the metal and the polymer can be investigated. Especially the quality of the connection between the two components and also defects can be characterised.

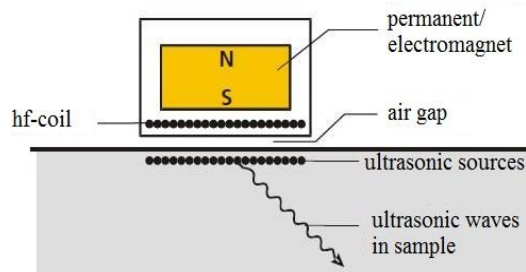


Fig. 6. Principle of an EMAT-probe [Source: F. Niese, Dissertation, 2010]

In Fig. 7 the signal curves for aluminium samples with and without bonding are compared. A sample with bonding is bonded to CFRP with a polymer. As can be seen there is a difference between samples with and without bonding. The ultrasonic signals are damped for the sample with bonding at times from 125 μ s to 180 μ s, which is an indication for a good bonding.

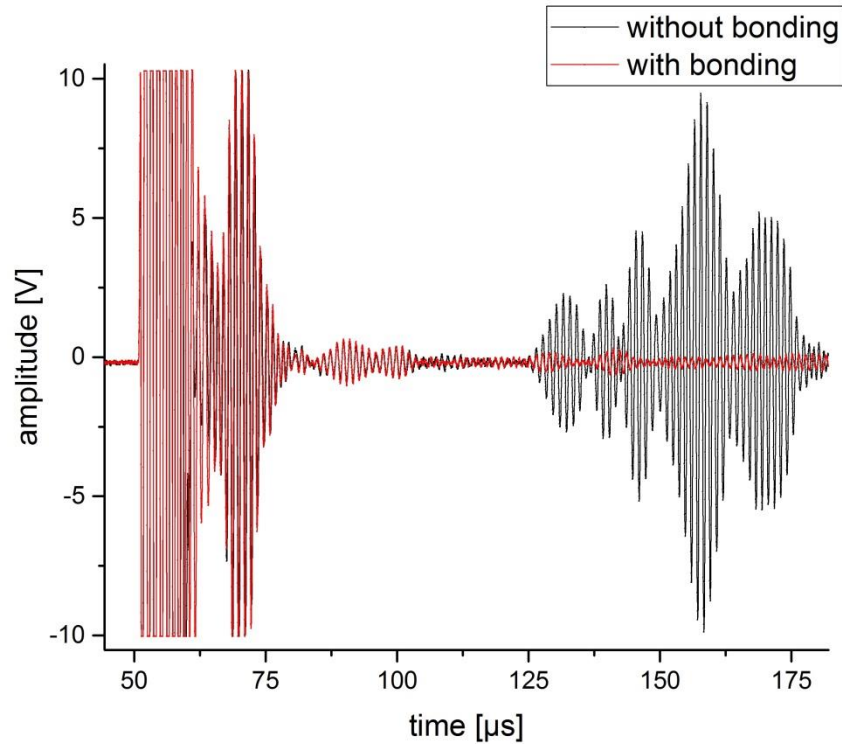


Fig. 7. EMAT measurement signal curves of samples with and without bonding

4. Conclusions and outlook

As shown in this work active and passive thermography as well as ultrasonic testing is well suited to characterise CFRP samples or aluminium-CFRP bonded samples. Artificial implemented defects can be characterised by thermography and bonded samples by ultrasonic testing with EMAT.

With passive thermography damage monitoring a good correlation between the spontaneous temperature increase due to fracture and the strain energy density or tensile strength respectively could be found for CFRP specimens containing different types of defects.

Investigating the fatigue properties, information on the accumulated irreversible strain is provided by the average sample temperature. By correlating the differential T-image and lock-in transformed image the information density on the lateral damage state was improved.

The combination of active and passive thermography enabled to identify weak points of the specimens, since the damage state could be characterised before, during and after mechanical testing. In further works hybrid samples with optimised geometry will be characterised. Also other nondestructive testing methods will be applied for a better characterisation of the hybrid samples.

Acknowledgement

The authors gratefully acknowledge the funding by Deutsche Forschungsgemeinschaft and also thank their colleagues from Fraunhofer IZFP Saarbrücken and their research partners from wbk at Karlsruher Institute of Technology and LKT at TU Dortmund.

References

- [1] Helfen Thomas, Nichtlinearer Ultraschall zur Charakterisierung von Ermüdungsschäden während der Hochfrequenz-Beanspruchung von C-Faser-Kunststoffverbunden, Universität des Saarlandes, Dissertation, 2014, p. 12-22
- [2] Amancio-Filho S.T., dos Santos J.F., Polymer Engineering and Science, p. 1461-1467, 2009
- [3] Kelly G., Composite Structures, 72, p. 119-129, 2006
- [4] Casas-Rodriguez J.P., Ashcroft I.A., Silberschmidt V.V., Delamination in adhesively bonded CFRP joints: Standard fatigue, impact-fatigue and intermittent impact, Composites Science and Technology 68 (2008) 2401–2409.
- [5] Rösner H., Netzelmann U., et. Al., Thermographic Materials Characterization, Springer, 2004, p. 246-285
- [6] Maldague X.P.V., Theory and Practice of Infrared Technology for Nondestructive Testing, John Wiley & Sons, Inc., 2001, p. 15-32
- [7] Roche J.M., et. Al., Proceedings on QNDE 2012, Denver U.S.A.
- [8] Chrysochoos A., Louche, H., International Journal of Engineering Science, 38, p. 1759-1788, 2000
- [9] Jegou L., et. Al., International Journal of Fatigue, 47, p. 259-267, 2013
- [10] Arif M.F., et. Al., Composites : Part B, 61, p. 55-65, 2014
- [11] Salzburger H.-J., Niese F., Dobmann G., Emat Pipe inspection with guided Waves, Welding in The World 56 (2012) 35-43